Altered Cerebral Energy Metabolism in Alzheimer's Disease: A PET Study

Hidenao Fukuyama, Masafumi Ogawa, Hiroshi Yamauchi, Shinya Yamaguchi, Jun Kimura, Yoshiaru Yonekura and Junji Konishi

Department of Neurology, Faculty of Medicine and Department of Radiology and Nuclear Medicine, Kyoto University, Kyoto, Japan

In an effort to better understand the metabolic basis for the reported decreases in regional cerebral cortex glucose metabolism in patients with Alzheimer's disease, glucose utilization oxygen consumption and regional cerebral blood flow were examined. **Methods:** Nine patients with Alzheimer's disease and nine age-matched normal controls were imaged using ^{18}F-labeled deoxyglucose and ^{15}O-labeled gases. **Results:** Regional analysis of the cerebral metabolic rate of glucose (CMRglu), cerebral metabolic rate of oxygen ($CMRO_2$) and cerebral blood flow (CBF) revealed that these values were significantly low in the frontal, parietal and temporal regions. The parietotemporal region had an abnormally high metabolic ratio ($CMRO_2$/CMRglu), while the frontal, sensorimotor and occipital visual cortices had a metabolic ratio similar to that of the normal controls. **Conclusions:** These findings suggest that the abnormal parietotemporal metabolism in Alzheimer's disease involves a metabolic shift from glycolytic to oxidative metabolism. This impairment of glucose degradation may be the basis for synoptic dysfunction underlying the impairment observed in Alzheimer's disease.

Key Words: Alzheimer's disease; parietotemporal metabolism; glucose metabolism

J Nucl Med 1994; 35:1–6

Abnormal reduction of metabolism in the parietotemporal region has been reported in the early stage of Alzheimer's disease (*1–3*), although no definite conclusions have been reached as to the pathophysiological significance of this metabolic derangement. Oxygen metabolism involves consumption of oxygen in the mitochondria through the tricarboxylic acid cycle, while glucose metabolism includes glucose consumption as lactate plus the mitochondrial catabolism of pyruvate to carbon dioxide. Thus, simultaneous measurement of oxygen and glucose metabolism allows assessment of the metabolic state of the brain, and the ratio of these two types of metabolism is an index of whether the brain depends on anaerobic or aerobic metabolism.

Neuropathological studies have suggested regional heterogeneity in the cortex of Alzheimer's patients with relative sparing of the primary sensorimotor and visual cortices, and selective damage to the parietotemporal lobes (*4–6*). We speculated that this pathological and morphological regionality reflects regional differences in the pathophysiology of Alzheimer's disease.

The aim of this study was to elucidate differences in energy metabolism among the various regions of the cerebral cortex using positron emission tomography (PET) in order to investigate the pathophysiological processes occurring in Alzheimer's disease.

PATIENTS AND METHODS

Patient Selection

We studied nine cases of Alzheimer's disease (mean age ± s.d.: 58.2 ± 8.3 yr; 7 males and 2 females), all of whom fulfilled the criteria for probable Alzheimer's disease proposed by NINCDS-ADRDA (*7*). Their disease was ranked as being in the first or second stage according to the clinical classification of Pearce (*8*). They had no abnormalities on magnetic resonance imaging except for brain atrophy, and had normal laboratory test results including syphilis serology, vitamin B12 levels and thyroid hormone levels. The age, sex, Hasegawa Dementia Rating Scale (*9*), Wechsler Adult Intelligence Scale and Hutchinski's ischemic score data are presented in Table 1. We excluded vascular dementia by magnetic resonance imaging or CT findings, and Hutchinski's ischemic score was less than 3 in all the patients.

Nine age- and sex-matched control patients (mean age: 46.6 ± 16.3 yr, Student's unpaired t-test, $p = 0.066$; 8 males and 1 female, chi-square test, $p > 0.05$) were also studied.

PET Procedure

PET Scanner and Scanning Method. The PET scanner was Positologica III (*10*). The best spatial resolution at full-width half-maximum was 7.6 mm in the center of the scan field of the cross-plane, with 192 bismuth germanate detectors per ring. This scanner had five rings located 16 mm apart, and therefore could obtain seven slices simultaneously. The slice thickness was 10 mm and the interval between the slices was 6 mm. We reconstructed a functional image consisting of 64 × 64 pixels, with each pixel measuring 2.5 × 2.5 mm. Cross-calibration between the

Received Jun. 4, 1993; revision accepted Sept. 29, 1993.

For correspondence and reprints contact: Dr. H. Fukuyama, Dept. of Neurology, Faculty of Medicine, Kyoto University, 54 Shogoin Kawahara-cho, Sakyo-ku, Kyoto, 606 Japan.

TABLE 1
Clinical and Psychometric Data of Alzheimer's Patients

Patient no.	Age (yr)	Sex	HDRS*	WAIS†			Hutchinski‡
				V	P	T	IS
1	58	M	18	64	60>	60>	1
2	55	M	20	95	60	81	1
3	69	M	19	66	90	74	2
4	46	F	17.5	94	60	77	1
5	54	M	19.5	82	60>	66	3
6	55	M	16	—§	—§	—§	2
7	63	M	7	60>	60>	60>	1
8	72	F	20	—§	—§	—§	1
9	52	M	16	114	92	87	2

*HDRS = Hasegawa Dementia Rating scale (full score is 31.5, a score of 20 or less indicates dementia).
†WAIS = Wechsler Adult Intelligence Scale; V = verbal; P = performance; and T = total intelligence quotient.
‡Hutchinski IS = Hutchinski Ischemic Score (4 or less indicates no ischemia).
§Study not performed.

scanner and the well counter and the cross-planes of the scanner was performed.

A blank scan was done before the patients were placed on the scanner table, and a transmission scan was performed using $^{68}Ga/^{68}Ge$ for absorption correction after patients were positioned in a specially molded headholder. CO_2 and O_2 labeled with ^{15}O were inhaled continuously at 370–555 MBq and 740–1110 MBq per minute, respectively. Oxygen-15-labeled CO was inhaled as a single dose of 2960 MBq. Arterial blood sampling was done three times per scan (5 min) (*11*), in addition to blood gas analysis. The pH of arterial blood influences the ionic state of various substances such as lactate which affects the amount of lactate loss from the brain (*12*) and influences the metabolic ratio, so special note of the arterial pH was taken during the examination. The physiological parameters during PET studies are presented in Table 2. No statistical differences between two groups were found for these variables by Student's unpaired t-test ($p > 0.05$) except for the O_2 content.

Immediately after the gas study, we intravenously administered 185 MBq of ^{18}F-labeled deoxyglucose. Arterial blood sampling was done just after administration and later at 30, 45, 60, 75 and 90 sec and at 2, 2.5, 3, 4, 5, 6, 8, 10, 15, 20, 30, 45 and 60 min. Brain scanning was started 45 min after the injection and emission data were collected for 15 min (*13*).

Examinations were done with eyes open and ears unplugged. Five Alzheimer's patients underwent both studies consecutively, while the other four Alzheimer's patients and the normal controls were examined on separate occasions within 1 mo. In the latter groups, the head position was fixed as similarly as possible for both scans using a customized headholder by a fast-hardening foam mold for each subject (*14*). However, we did not compare the steadiness of the data obtained by serial examinations on the same day or separate examinations on different days.

Calculations. Cerebral blood flow (CBF), the cerebral metabolic rate of oxygen ($CMRO_2$) and the oxygen extraction fraction (OEF) were obtained by the steady-state method using ^{15}O-labeled gases (*15*). Cerebral blood volume (CBV) was calculated by the bolus inhalation of ^{15}O-labeled carbon monoxide and was incorporated in the correction of vascular space for $CMRO_2$ and OEF (*16*).

The cerebral metabolic rate of glucose (CMRglu) was calculated by Phelps' autoradiographic method using ^{18}F-labeled deoxyglucose (*17*). The incorporated metabolic rate constants were K1*

TABLE 2
Physiological Parameters in Alzheimer's Patients and Normal Controls

	Alzheimer's disease	Normal controls
pH	7.39 ± 0.04	7.39 ± 0.03
pCO_2 (mmHg)	41.47 ± 3.07	39.80 ± 3.02
PO_2 (mmHg)	91.40 ± 8.33	102.31 ± 21.17
Hb (mg/dl)	12.73 ± 1.04	13.88 ± 1.34
O_2 content (vol%)	17.20 ± 1.57*	19.22 ± 1.90
Ht (%)	37.60 ± 2.64	40.50 ± 3.95
Glucose (mg/dl)	88.67 ± 6.89	86.00 ± 4.50
Blood pressure	137/74	135/73

Data represent the mean ± s.d. except for blood pressure.
Blood pressure is mean systolic pressure/mean diastolic pressure.
There are no significant differences between the Alzheimer's group and normal controls, except for the O_2 content.

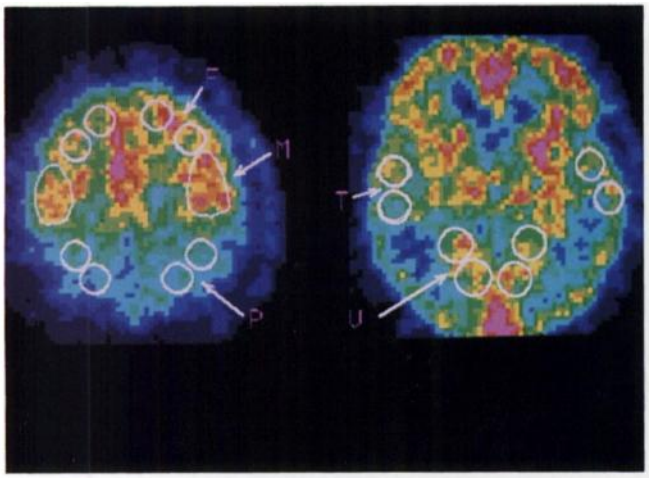

FIGURE 1. A CBF image from an Alzheimer's patient and overlaid ROIs. The ROIs are delineated by white lines. Abbreviations: F = frontal; M = sensorimotor; P = parietal; V = visual; and T = temporal cortex.

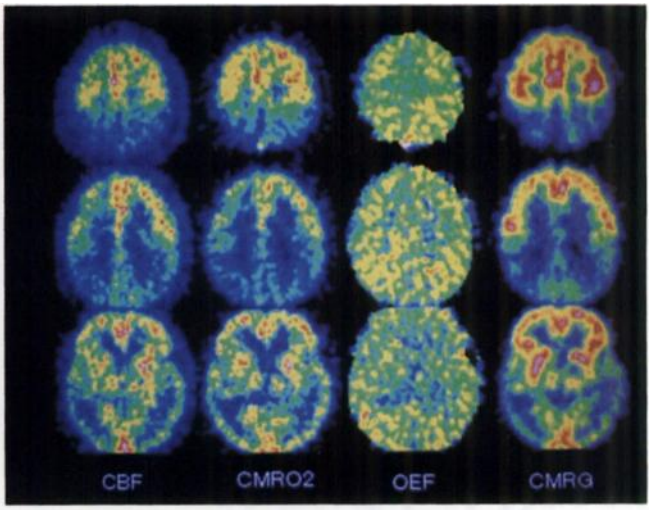

FIGURE 2. A 55-yr-old male with Alzheimer's disease. From left to right, the columns show CBF, $CMRO_2$, OEF and CMRglu. Significant reduction of CBF and CMRglu and moderate reduction of $CMRO_2$ were noted in the parietotemporal region; a slight increase in OEF was also observed in the same region.

= 0.102, k2* = 0.130 and k3* = 0.062, and the lumped constant was 0.52 (*18*).

Data Analysis and Statistical Analysis

Regions of interest (ROIs) were determined on the cortical ribbon in the CBF image (Fig. 1). We placed two to three circular ROIs, which consisted of 11 pixels representing 68.75 mm^2, in every region. The ROIs included the frontal, parietal and temporal regions covering the anterior and posterior association cortices. In addition, we placed one irregular and two circular ROIs over the sensorimotor and occipital visual cortices respectively. These regions possessed a high CBF compared to the surrounding areas in Alzheimer's patients and were easily identified. In normal controls, the primary cortical regions and the association cortices were visually identified by referring to the corresponding magnetic resonance images. The same ROIs were transferred to the $CMRO_2$, OEF, CBV and CMRglu images.

After regional circulatory and metabolic parameters were obtained, the metabolic ratio (MR) was calculated by dividing $CMRO_2$ by CMRglu on a molar basis.

The calculated data were compared for their regional differences between patients with Alzheimer's disease and normal controls by analysis of variance with post hoc Bonferroni-corrected t-tests. A probability value less than 0.05 was considered to indicate significant difference.

RESULTS

The nine Alzheimer's patients had a high MR in the parietal and temporal cortices when compared to the normal controls ($p < 0.05$). The primary sensorimotor and visual cortices as well as the frontal cortex had relatively low MR values compared to the parietal and temporal

TABLE 3
Regional Cerebral Blood Flow, Oxygen Metabolism, Glucose Metabolism and Metabolic Ratio in Alzheimer's Patients and Normal Controls

Region		CBF	$CMRO_2$	OEF	CMRglu	MR
Frontal	Alz	28.88 ± 3.47*	81.41 ± 16.43†	0.43 ± 0.053	27.02 ± 5.73*	3.07 ± 0.57
	Nor	37.34 ± 3.74	105.65 ± 25.69	0.39 ± 0.024	36.06 ± 3.95	2.95 ± 0.77
Sensori	Alz	33.29 ± 4.81	92.31 ± 19.40	0.43 ± 0.051	32.05 ± 7.12	2.91 ± 0.37
Motor	Nor	37.22 ± 3.37	111.36 ± 25.19	0.40 ± 0.030	36.21 ± 4.35	3.12 ± 0.85
Visual	Alz	35.63 ± 5.78	97.75 ± 24.88	0.44 ± 0.046	31.28 ± 7.31	3.15 ± 0.59
	Nor	38.18 ± 2.90	111.36 ± 19.79	0.43 ± 0.033	36.63 ± 3.74	3.06 ± 0.54
Parietal	Alz	23.79 ± 3.87*	70.28 ± 12.56*	0.46 ± 0.050	18.67 ± 5.08*	3.91 ± 0.81†
	Nor	38.14 ± 4.53	115.47 ± 26.19	0.43 ± 0.030	36.65 ± 3.73	3.13 ± 0.45
Temporal	Alz	28.23 ± 5.63*	81.17 ± 17.89*	0.45 ± 0.066	21.11 ± 5.37*	3.96 ± 0.82†
	Nor	41.17 ± 6.69	117.69 ± 31.60	0.41 ± 0.024	37.51 ± 3.16	3.11 ± 0.63

*$p < 0.01$ against normal control value.
†$p < 0.05$ against normal control value of a corresponding region.
Data were expressed as mean ± s.d.
CBF = cerebral blood flow (ml/100 g/min); $CMRO_2$ = cerebral metabolic rate of oxygen (μmole/100 g/min); OEF = oxygen extraction fraction; CMRglu = cerebral metabolic rate of glucose (μmole/100 g/min); and MR = metabolic ratio.

regions and showed no significant differences between Alzheimer's patients and normal controls (Table 3).

CBF showed fronto-temporo-parietal reduction in Alzheimer's disease ($p < 0.01$), while the visual and sensorimotor cortices had normal CBF.

Investigation of oxygen metabolism revealed that the $CMRO_2$ was decreased in the frontal ($p < 0.05$), temporal ($p < 0.01$) and parietal regions ($p < 0.01$) of the patients with Alzheimer's disease, while the OEF was slightly increased, but none of the differences were significant. The visual and sensorimotor cortices showed similar $CMRO_2$ values in the patients with Alzheimer's disease and the normal controls.

In Alzheimer's disease, the CMRglu was reduced in the parietal and temporal regions as well as in the frontal region when compared to the normal controls ($p < 0.01$). However, primary cortices showed no significant reduction in Alzheimer's disease when compared to the normal controls.

A representative 55-yr-old Alzheimer's disease patient is presented in Figure 2. A marked decreased of CMRglu as well as CBF can be noted in the parietotemporal region, while the suppression of $CMRO_2$ is moderate.

DISCUSSION

Measurement of oxygen metabolism was performed by the steady-state method, so it represents the energy metabolism of the mitochondria. One mole of glucose contains 6 moles of carbon atoms, so the ratio between oxygen and glucose metabolism would be 6, if complete glucose degradation occurred in the mitochondria and no glucose was lost from the brain. The metabolic ratio obtained from PET data was about 5 in the normal controls (*19,20*) and apparently lower than the stoichiometric value or that obtained by the Kety-Schmidt method where 5 is a reportedly normal value (*21*).

The present study showed that the MR was 3 in the normal controls and in the frontal, sensorimotor or occipital visual cortex of the Alzheimer's patients. Therefore, the ratio was low compared to other values reported with PET. According to a transport study, the net efflux of lactate from the brain is 4 μmole/100 g/min (*12*). Since the standard value of CMRglu was 30 μmole/100 g/min, about 10% of the glucose transported into the brain was washed out in the form of lactate, and this glucose loss was not sufficient to account for the remarkably low MR. In fact, the calculated MR considering this lactate loss is 5.4. Another reason for the discrepancy is that the steady-state method underestimates oxygen metabolism.

In calculating CBF, the underestimation of high flows has been reported to be an intrinsic problem of the steady-state method (*22*), but because Alzheimer's brains do not have such high blood flow, its underestimation would be expected. The oxygen metabolic rate we obtained was low compared to the standard value of 150 μmole/100 g/min obtained for the cortex using the classical arteriovenous difference (*23*). The oxygen metabolic rate was obtained by multiplying CBF, OEF and arterial oxygen content. Arterial oxygen content was low in the Alzheimer's group when compared to normal controls (Table 2), who showed no marked deviation from the standard value. The OEF was within the normal range in both groups, therefore, the low $CMRO_2$ value could be partly ascribed to the low CBF. In addition, a previous study (*24*) which used a lumped constant to adjust the metabolic ratio to 5.6 consequently employed a high lumped constant of 0.75. However, we used a value of 0.52, as reported by Reivich et al. (*18*). This made the CMRglu value larger when compared to the use of a large lumped constant. Thus, if we had adopted a larger lumped constant, such as 0.75, the MR value in normal controls would be around 4.5. These factors contributed to the relatively low MR obtained in our PET study.

In contrast to the classical pathological concept about Alzheimer's disease (a diffuse and almost uniform degenerative process), quantitative pathological studies have indicated regional differences of involvement (*4–6*). The most affected areas were the temporal, frontal and parietal lobes, while the sensorimotor, calcarine and anterior cingulate areas being notably spared until the very late stages. This finding suggested that the association cortex was the most severely affected area, so we determined ROIs for the association cortex and the primary cortex (sensorimotor and visual cortices) as a control area.

We found that the MR of the parietal and temporal lobes was significantly higher in Alzheimer's disease compared to the control group, while the sensorimotor and visual cortices had similar MR values in both groups. This difference was considered to reflect the changes of energy metabolism in the parietotemporal region in Alzheimer's disease. Total energy consumption was reduced in the parietotemporal region in the Alzheimer's disease patients and the ratio of glycolytic and oxidative metabolism was altered with energy consumption shifting from anaerobic to aerobic.

The presence of a severe deficit of cholinergic cortical projections from the nucleus basalis of Mynert has been proved in Alzheimer's disease (*25*), and cholinergic deficiency in the neocortex correlated with the intellectual deterioration observed in psychometric tests (*26*). A disturbance of glycolytic metabolism would lead to decreased production of acetyl Co-A, following reduced acetylcholine production. Thus, the decreased glucose catabolism in the parietotemporal region provides supportive evidence for acetylcholine depletion in Alzheimer's brains.

Oxygen metabolism was reduced in the temporoparietal region in patients with mild degenerative dementia (*27*). This tendency was reflected in the present study and oxygen metabolism was not so severely affected in the Alzheimer's brains and glucose utilization was more specifically impaired (*28,29*). Measurement of whole-brain oxygen and glucose metabolism using the Kety-Schmidt technique showed that the predominant abnormality in incipient late-

onset Alzheimer's disease was a 45% reduction in cerebral glucose utilization, whereas the $CMRO_2$ was diminished by only 18%, and a severe imbalance between oxygen and glucose utilization was obvious (*30*). Our present results support this finding and also suggest that the metabolic imbalance is more conspicuous in specific areas such as the parietotemporal region. The following possibilities can be suggested to explain this pathophysiology.

First, a decrease of specific proteins in the glucose degradation pathway like the glucose transporter or a functional disturbance of enzymes such as hexokinase (a rate-limiting enzyme in glycolysis) (*31*) might lead to a disturbance of glucose degradation. We previously analyzed the metabolic rate constants in Alzheimer's disease by dynamic PET scanning and found a reduction of k3 (hexokinase activity) in the parietal region (*13*). Furthermore, the quantity of glucose transporter in Alzheimer's brains is reported to be reduced compared to the normal controls (*32*). PET studies have also disclosed a decrease of K1 in the frontal, temporal and parietal regions, suggesting reduced glucose transporter activity in those areas (*13,33*). Therefore, glucose metabolism is compromised to some extent in Alzheimer's disease.

Second, synaptic dysfunction in the parietotemporal cortex could be responsible. Neurohistochemical studies have shown far milder cell loss compared with the extensive synaptic disruption noted in the parietotemporal region in Alzheimer's disease (*34,35*). A histochemical study on pyruvate dehydrogenase and glucose transporter (*36*) has indicated that anaerobic glucose degradation mostly occurs in the dendrites or axons, while aerobic oxygen metabolism is localized to the perikarya, chiefly the mitochondria. Therefore, synaptic dysfunction would be represented as a decrease in glucose degradation. It can be suggested that the reduced glucose utilization in Alzheimer's disease is related to neuronal dysfunction originating from synaptic damage due to some pathological process intrinsic to Alzheimer's disease.

However, the following questions remain unsettled about this hypothesis. The elevated MR in the parietotemporal region in Alzheimer's disease indicates that the acetate moiety is supplied from some other source than glucose. Since the MR rises with advancing age, ketone body oxidation is suspected to be involved (*37*). There seems to be no biochemical evidence indicating increased alternative substrate consumption such as ketone bodies, fatty acids or glutamate, by the tricarboxylic acid cycle in Alzheimer's disease. The other problem is that frontal hypometabolism of oxygen and glucose was apparent, but no MR elevation was observed. The most plausible explanation is that glucose metabolism in the frontal lobe was not so severely depressed compared with that in the temporal and parietal lobes (27 versus 21.1 and 18.7 μmole/100 g/min) because our patients were in the early stage of Alzheimer's disease, although the difference of CMRglu between the control and Alzheimer's frontal lobe was significant ($p < 0.01$). The late stage of Alzheimer's disease may well feature an elevated MR in the frontal cortex as well as the parietotemporal region.

In conclusion, these data support the hypothesis that the primary pathophysiological mechanism in the early stage of Alzheimer's disease is synaptic dysfunction in the association cortices based on impairment of glucose degradation.

ACKNOWLEDGMENTS

The authors thank Drs. Y. Iwasaki, N. Sadatoh, Y. Magata, H. Saji, T. Miyoshi and T. Doi for their support and advice.

REFERENCES

1. Friedland RP, Brun A, Budinger TF. Pathological and positron emission tomographic correlations in Alzheimer's disease. *Lancet* 1985;1:228.
2. Cutler NR, Haxby JV, Duara R, et al. Clinical history, brain metabolism, and neuropsychological function in Alzheimer's disease. *Ann Neurol* 1985; 18:298–309.
3. De Leon MJ, Ferris SH, George AE, et al. Computed tomography and positron emission transaxial tomography evaluations of normal aging and Alzheimer's disease. *J Cereb Blood Flow Metab* 1983;3:391–394.
4. Brun A, Englund E. Regional pattern of degeneration in Alzheimer's disease: neuronal loss and histopathological grading. *Histopathology* 1981;5: 549–564.
5. Pearson RCA, Esiri MM, Hiorns RW, Wilcock GK, Powell TPS. Anatomical correlates of the distribution of the pathological changes in the neocortex in Alzheimer disease. *Proc Natl Acad Sci USA* 1985;82:4531–4534.
6. Rogers J, Morrison JH. Quantitative morphology and regional and laminal distributions of senile plaques in Alzheimer's disease. *J Neurosci* 1985;5: 2801–2808.
7. McKhann G, Drachman D, Flostein M, Katzman R, Price D, Stadlan EM. Clinical diagnosis of Alzheimer's disease: report of the NINCDS-ADRDA work group under the auspices of department of health and human services task force on Alzheimer's disease. *Neurology* 1984;34:939–944.
8. Pearce JMS. *Dementia: a clinical approach*. Oxford: Blackwell Scientific Publications; 1984:27–31.
9. Hasegawa K, Inoue K, Moriya K. An investigation of dementia rating scale for the elderly (in Japanese). *Seisin Igaku* 1974;16:965–969.
10. Senda M, Tamaki N, Yonekura Y, et al. Performance characteristics of Positologica III: a whole-body positron emission tomograph. *J Comput Assist Tomogr* 1985;9:940–946.
11. Fukuyama H, Kameyama H, Harada K, et al. Thalamic tumors invading the brain stem produce crossed cerebellar diaschisis demonstrated by PET. *J Neurol Neurosurg Psychiatry* 1986;49:524–528.
12. Knudsen GM, Paulson OB, Hertz MM. Kinetic analysis of the human blood-brain barrier transport of lactate and its influence by hypercapnia. *J Cereb Blood Flow Metab* 1991;11:581–586.
13. Fukuyama H, Kameyama M, Harada K, et al. Glucose metabolism and rate constants in Alzheimer's disease examined with dynamic positron emission tomography scan. *Acta Neurol Scand* 1989;80:307–313.
14. Kearfott KJ, Junck L, Rottenberg DA. A new headholder for PET, CT and NMR imaging. *J Comput Assist Tomogr* 1983;8:1217–1220.
15. Frackowiak RSJ, Lenzi G-L, Jones T, Heather JD. Quantitative measurement of regional cerebral blood flow and oxygen metabolism in man using ^{15}O and positron emission tomography: theory, procedure, and normal values. *J Comput Assist Tomogr* 1980;4:727–736.
16. Lammertsma AA, Jones T. Correction for the presence of intravascular oxygen-15 in the steady-state technique for measuring regional oxygen extraction ratio in the brain: 1. Description of the method. *J Cereb Blood Flow Metab* 1983;3:416–424.
17. Phelps ME, Huang SC, Hoffman EJ, Selin C, Sokoloff L, Kuhl DE. Tomographic measurement of local cerebral glucose metabolic rate in humans with (F-18)2-fluoro-2-deoxy-D-glucose: validation of method. *Ann Neurol* 1979;6:371–388.
18. Reivich M, Alavi A, Wolf A, et al. Glucose metabolic rate kinetic model parameter determination in humans: the lumped constants and rate constants for [^{18}F]Fluorodeoxyglucose and [^{11}C]deoxyglucose. *J Cereb Blood Flow Metab* 1985;5:179–192.
19. Baron JC, Rougemont D, Soussaline F, et al. Local interrelationships of cerebral oxygen consumption and glucose utilization in normal subjects and

in ischemic stroke patients: a positron tomography study. *J Cereb Blood Flow Metab* 1984;4:140–149.
20. Hatazawa J, Ito M, Matsuzawa T, Ido T, Watanuki S. Measurement of the ratio of cerebral oxygen consumption of glucose utilization by positron emission tomography: its consistency with the values determined by the Kety-Schmidt method in normal volunteers. *J Cereb Blood Flow Metab* 1988;8:426–432.
21. Dastur DK. Cerebral blood flow and metabolism in normal aging, pathological aging, and senile dementia. *J Cereb Blood Flow Metab* 1985;5:1–9.
22. Huang S-C, Mahoney K, Phelps ME. Quantitation in positron emission tomography: 8. Effects of nonlinear parameter estimation on functional images. *J Comput Assist Tomogr* 1987;11:314–325.
23. Allen N. Oxidative metabolism of brain tumors. *Progr Exp Tumor Res* 1972;17:192–209.
24. Frackowiak RSJ, Herold S, Petty RKH, Morgan-Hughes JA. The cerebral metabolism of glucose and oxygen measured with positron tomography in patients with mitochondrial diseases. *Brain* 1988;111:1009–1024.
25. Whitehouse PJ, Price DL, Clark AW, Coyle JT, DeLong MR. Alzheimer's disease: evidence for selective loss of cholinergic neurons in the nucleus of basalis. *Ann Neurol* 1981;10:122–126.
26. Perry EK, Tomlinson BE, Blessed G, Bergmann K, Gibson PH, Perry RH. Correlation of cholinergic abnormalities with senile plaques and mental test scores in senile dementia. *Br J Med* 1978;2:1457–1459.
27. Frackowiak RSJ, Pozzilli C, Legg NJ, et al. Regional cerebral oxygen supply and utilization in dementia. A clinical and physiological study with oxygen-15 and positron tomography. *Brain* 1981;104:753–778.
28. Foster NL, Chase TN, Fedio P, Patronas NJ, Brooks RA, Di Chiro G. Alzheimer's disease: focal cortical changes shown by positron emission tomography. *Neurology* 1983;33:961–965.
29. Friedland RP, Budinger TF, Ganz E, et al. Regional cerebral metabolic alterations in dementia of the Alzheimer type: positron emission tomography with [^{18}F]fluorodeoxyglucose. *J Comput Assist Tomogr* 1983;7:590–598.
30. Hoyer S, Nitsch R, Oesterreich K. Predominant abnormality in cerebral glucose utilization in late-onset dementia of the Alzheimer type: a cross-sectional comparison against advanced late-onset and incipient early-onset cases. *J Neural Transm Park Dis Dement Sect* 1991;3:1–14.
31. Hawkins RA, Mans AM. Intermediary metabolism of carbohydrates and other fuels. In: Lajtha A, ed. *Handbook of neurochemistry, volume 3.* New York: Plenum Press; 1983:259–294.
32. Kalaria RN, Harik SI. Reduced glucose transporter at the blood-brain barrier and in cerebral cortex in Alzheimer disease. *J Neurochem* 1989;53: 1083–1088.
33. Jagust WJ, Seab JP, Huesman RH, et al. Diminished glucose transport in Alzheimer's disease: dynamic PET studies. *J Cereb Blood Flow Metab* 1991;11:323–330.
34. Maslia E, Iimoto DS, Saitoh T, Hansen LA, Terry RD. Increased immunoreactivity of brain spectrin in Alzheimer disease: a marker for synapse loss? *Brain Res* 1990;531:36–44.
35. Hamos JE, DeGennaro LJ, Drachman DA. Synaptic loss in Alzheimer's disease and other dementias. *Neurology* 1989;39:355–361.
36. Bagley PR, Tucker SP, Nolan C, et al. Anatomical mapping of glucose transporter protein and pyruvate dehydrogenase in rat brain: an immunogold study. *Brain Res* 1989;499:214–224.
37. Kuhl DE, Metter EJ, Riege WH, Phelps ME. Effects of human aging on patterns of local cerebral glucose utilization determined by the [^{18}F]fluorodeoxyglucose method. *J Cereb Blood Flow Metab* 1982;2:163–171.